

# USBL/INS Tightly-Coupled Integration Technique for Underwater Vehicles

M. Morgado, P. Oliveira, C. Silvestre, and J.F. Vasconcelos\*  
Instituto Superior Técnico  
Institute for Systems and Robotics  
Av. Rovisco Pais, 1, 1049-001, Lisbon, Portugal  
{marcomorgado,pjcro,cjs,jfvasconcelos}@isr.ist.utl.pt

**Abstract** - *This paper presents a new Ultra-Short Baseline (USBL) tightly-coupled integration technique to enhance error estimation in low-cost strapdown Inertial Navigation Systems (INSs) with application to underwater vehicles. In the proposed strategy the acoustic array spatial information is directly exploited resorting to the Extended Kalman Filter implemented in a direct feedback structure. The determination and stochastic characterization of the round trip travel time are obtained resorting to pulse detection matched filters of acoustic signals modulated using spread-spectrum Code Division Multiple Access (CDMA). The performance of the overall navigation system is assessed in simulation and compared with a conventional loosely-coupled solution that consists of solving separately the triangulation and sensor fusion problems. From the simulation results it can be concluded that the proposed technique enhances the position, orientation, and sensors biases estimates accuracy.*

**Keywords:** Sensor Modeling, Tracking and surveillance, Fusion architecture, Application of fusion.

## 1 Introduction

Worldwide, there has been an increasing interest in the use of underwater vehicles to expand the ability to accurately survey large ocean areas. Future missions at sea include environmental monitoring and surveillance, underwater inspection of estuaries, harbors, and pipelines, and geological and biological surveys [1]. The use of these robotic platforms requires low-cost, compact, high performance robust navigation systems, that can accurately estimate the vehicle's position and attitude. These facts raised, in the last years, the robotics scientific community awareness towards the development of accurate navigation systems [2, 3].

Inertial Navigation Systems (INS) provide self-contained passive means for three-dimensional posi-

tioning in open ocean with excellent short-term accuracy. However, unbounded positioning errors induced by the uncompensated rate gyro and accelerometer errors degrade the INS accuracy over time. This degradation is more severe for low-cost INS systems, requiring aiding sensors and more complex filtering techniques in order to meet performance specifications and to tackle noise and bias effects. New onboard aiding compensation techniques and multiple inertial sensor error models have been recently taken into account in the navigation system's structure, to enhance its performance and robustness. Among a diverse set of promising techniques, an Extended Kalman Filter (EKF) implemented in a direct feedback configuration, allows to estimate position, velocity, orientation, and inertial sensor biases errors [4].

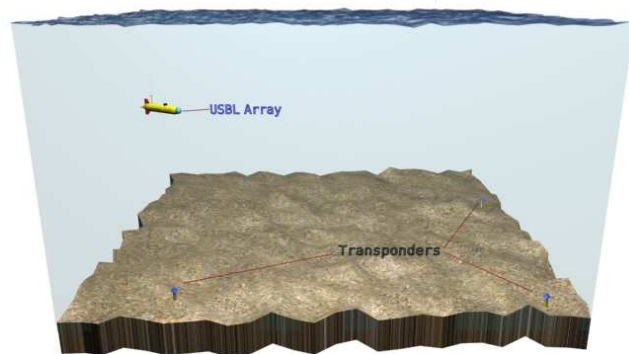


Figure 1: Mission scenario

This paper presents a new Ultra-Short Baseline (USBL) tightly-coupled integration technique to enhance error estimation in low-cost strapdown INS with application to underwater vehicles. In the proposed navigation architecture, the USBL acoustic array is installed onboard the vehicle to avoid the extensive use of an acoustic communication link between the vehicle and the reference station. In the paper it is assumed that the USBL provides either the range, azimuth and elevation or the round trip travel time to each of the array transducers. The USBL array interrogates the transponders located in known positions of the vehicle's mission area as illustrated in Figure 1.

Typical USBL/INS integration techniques, usually named loosely-coupled, rely on solving separately the

\*This work was partially supported by the FCT POSI programme under framework QCA III and by the project PDCT/MAR/55609/2004 - RUMOS of the FCT. The work of J.F. Vasconcelos was supported by a PhD Student Scholarship, SFRH/BD/18954/2004, from the Portuguese FCT POCTI programme.

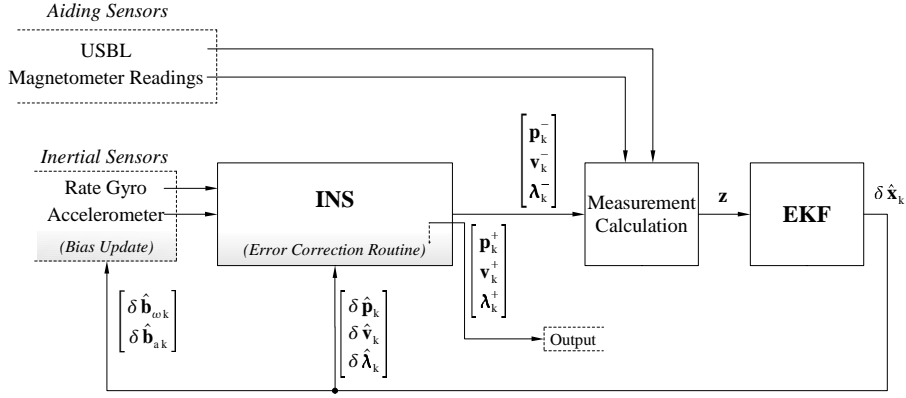


Figure 2: Navigation System Block Diagram

triangulation and sensor fusion problems, not taking into account the acoustic array geometry in the navigation system. The new proposed tightly-coupled USBL/INS integration strategy exploits directly the acoustic array spatial information, resorting to an EKF in a direct feedback configuration.

The paper is organized as follows: Section 2 briefly discusses the INS structure and algorithm adopted in this work. The main contribution of this paper is presented in Section 3, where the observation equations for the new USBL/INS integration strategy are derived. A solution for the classical strategy is also presented for benchmarking purposes. Comparison results of both strategies are presented in Section 4. Finally, Section 5 provides concluding remarks on the subject and comments on future work.

## 2 Aided Inertial Navigation System

This section describes the navigation system architecture, depicted in Figure 2. The INS is the backbone algorithm that performs attitude, velocity and position numerical integration from rate gyro and accelerometer triads data, rigidly mounted on the vehicle structure (strapdown configuration). The non-ideal inertial sensor effects due to noise and bias are dynamically compensated by the EKF to enhance the navigation system's performance and robustness. Position, velocity, attitude and bias compensation errors are estimated by introducing the aiding sensors data in the EKF, and are thus compensated in the INS according to the direct-feedback configuration shown in the figure.

### 2.1 Inertial Navigation System

For highly maneuverable vehicles, the INS numerical integration must properly address the angular, velocity and position high-frequency motions, referred to as coning, sculling, and scrolling respectively, to avoid estimation errors buildup. The INS multi-rate approach, based on the work detailed in [5, 6], computes the dynamic angular rate/acceleration effects using high-speed, low order algorithms, whose output is periodi-

cally fed to a moderate-speed algorithm that computes attitude/velocity resorting to exact, closed-form equations. Applications within the scope of this paper are characterized by confined mission scenarios and limited operational time allowing for a simplification of the frame set to Earth and Body frames and the use of an invariant gravity model without loss of precision.

The inputs provided to the inertial algorithms are the integrated inertial sensor output increments

$$\begin{aligned} \mathbf{v}(\tau) &= \int_{t_{k-1}}^{\tau} {}^B \mathbf{a}_{SF} dt \\ \boldsymbol{\alpha}(\tau) &= \int_{t_{k-1}}^{\tau} \boldsymbol{\omega} dt \end{aligned}$$

where  ${}^B \mathbf{a}_{SF}$  and  $\boldsymbol{\omega}$  represent the accelerometer and rate gyro readings, respectively. The inertial sensor readings are corrupted by zero mean white noise  $\mathbf{n}$  and random walk bias,  $\dot{\bar{\mathbf{b}}} = \mathbf{n}_b$ , yielding

$$\begin{aligned} {}^B \mathbf{a}_{SF} &= {}^B \bar{\mathbf{a}} + {}^B \bar{\mathbf{g}} - \delta \mathbf{b}_a + \mathbf{n}_a \\ \boldsymbol{\omega} &= \bar{\boldsymbol{\omega}} - \delta \mathbf{b}_\omega + \mathbf{n}_\omega \end{aligned}$$

where  $\delta \mathbf{b} = \mathbf{b} - \bar{\mathbf{b}}$  denotes bias compensation error,  $\bar{\mathbf{b}}$  is the nominal bias,  $\mathbf{b}$  is the compensated bias,  ${}^B \bar{\mathbf{g}}$  is the nominal gravity vector, and the subscripts  $a$  and  $\omega$  identify accelerometer and rate gyro quantities, respectively.

The attitude moderate-speed algorithm computes body attitude in Direction Cosine Matrix (DCM) form

$${}_{B_k}^{B_k} \mathbf{R}(\boldsymbol{\lambda}_k) = \mathbf{I}_{3 \times 3} + \frac{\sin \|\boldsymbol{\lambda}_k\|}{\|\boldsymbol{\lambda}_k\|} [\boldsymbol{\lambda}_k \times] + \frac{1 - \cos \|\boldsymbol{\lambda}_k\|}{\|\boldsymbol{\lambda}_k\|^2} [\boldsymbol{\lambda}_k \times]^2 \quad (1)$$

where  $\|\cdot\|$  represents the Euclidean norm,  $\{B_k\}$  is the Body frame at time  $k$  and  ${}_{B_k}^{B_k} \mathbf{R}(\boldsymbol{\lambda}_k)$  is the rotation matrix from  $\{B_k\}$  to  $\{B_{k-1}\}$  coordinate frames, parameterized by the rotation vector  $\boldsymbol{\lambda}_k$ . The rotation vector updates are formulated as

$$\boldsymbol{\lambda}_k = \boldsymbol{\alpha}_k + \boldsymbol{\beta}_k$$

in order to denote angular integration and coning attitude terms  $\boldsymbol{\alpha}_k$  and  $\boldsymbol{\beta}_k$ , respectively. The attitude high-speed algorithm computes  $\boldsymbol{\beta}_k$  as a summation of the high-frequency angular rate vector changes using simple, recursive computations [5], providing high-accuracy results.

Using the equivalence between strapdown attitude and velocity/position algorithms [7], the same multi-rate approach is applied [6] to compute exact velocity updates at moderate-speed

$$\mathbf{v}_k = \mathbf{v}_{k-1} + \frac{E}{B_{k-1}} \mathbf{R} \Delta^{B_{k-1}} \mathbf{v}_{SF\ k} + \Delta \mathbf{v}_{G/Cor\ k}$$

where  $\Delta^{B_{k-1}} \mathbf{v}_{SF\ k}$  is the velocity increment related to the specific force, and  $\Delta \mathbf{v}_{G/Cor\ k}$  represents the velocity increment due to gravity and Coriolis effects [6]. The term  $\Delta^{B_{k-1}} \mathbf{v}_{SF\ k}$  also accounts for high-speed velocity rotation and high-frequency dynamic variations due to angular rate vector rotation, yielding

$$\Delta^{B_{k-1}} \mathbf{v}_{SF\ k} = \mathbf{v}_k + \Delta \mathbf{v}_{rot\ k} + \Delta \mathbf{v}_{scul\ k}$$

where  $\Delta \mathbf{v}_{rot\ k}$  and  $\Delta \mathbf{v}_{scul\ k}$  are the rotation and sculling velocity increments respectively, computed by the high-frequency algorithms.

Interestingly enough, a standard low-power consumption DSP based hardware architecture is sufficient for running the INS algorithms using maximal computational accuracy at high execution rates. This allows to use maximal precision so that computational accuracy of the INS output is only diminished by the inertial sensors noise and biases effects.

Readers not familiarized with INS algorithms are referred to [5, 6, 8] for further details.

## 2.2 Extended Kalman Filter

The EKF error equations, based on perturbational rigid body kinematics, were brought to full detail by Britting [8], and are applied to local navigation by modeling the position, velocity, attitude and bias compensation errors dynamics, respectively

$$\begin{cases} \delta \dot{\mathbf{p}} = \delta \dot{\mathbf{v}} \\ \delta \dot{\mathbf{v}} = -\mathcal{R} \delta \mathbf{b}_a - [\mathcal{R}^B \mathbf{a}_{SF} \times] \delta \boldsymbol{\lambda} + \mathcal{R} \mathbf{n}_a \\ \delta \dot{\boldsymbol{\lambda}} = -\mathcal{R} \delta \mathbf{b}_\omega + \mathcal{R} \mathbf{n}_\omega \\ \delta \dot{\mathbf{b}}_a = -\mathbf{n}_{b_a} \\ \delta \dot{\mathbf{b}}_\omega = -\mathbf{n}_{b_\omega} \end{cases} \quad (2)$$

where the position and velocity linear errors are defined, respectively by

$$\delta \mathbf{p} = \mathbf{p} - \bar{\mathbf{p}} \quad (3)$$

$$\delta \mathbf{v} = \mathbf{v} - \bar{\mathbf{v}} \quad (4)$$

matrix  $\mathcal{R}$  is the shorthand notation for Body to Earth coordinate frames rotation matrix,  $\frac{E}{B} \mathbf{R}$ , and the attitude error rotation vector  $\delta \boldsymbol{\lambda}$  is defined by  $\mathbf{R}(\delta \boldsymbol{\lambda}) \triangleq \mathcal{R} \bar{\mathcal{R}}'$ , and bears a first order approximation

$$\mathbf{R}(\delta \boldsymbol{\lambda}) \simeq \mathbf{I}_{3 \times 3} + [\delta \boldsymbol{\lambda} \times] \Rightarrow [\delta \boldsymbol{\lambda} \times] \simeq \mathcal{R} \bar{\mathcal{R}}' - \mathbf{I}_{3 \times 3} \quad (5)$$

of the DCM form expressed in (1). In particular, the proposed error filter underlying model (2) includes the sensor's noise characteristics directly in the covariance matrices of the EKF and allows for attitude estimation using an unconstrained, locally linear and non-singular attitude parameterization.

Once computed, the EKF error estimates are fed into the INS error correction routines as depicted in

Figure 2. The attitude estimate,  $\mathcal{R}_k^-$ , is compensated using the rotation matrix  $\mathbf{R}(\delta \boldsymbol{\lambda})$  definition, which yields

$$\mathcal{R}_k^+ = \mathbf{R}'_k(\delta \hat{\boldsymbol{\lambda}}_k) \mathcal{R}_k^-$$

where  $\mathbf{R}'_k(\delta \hat{\boldsymbol{\lambda}}_k)$  is parameterized by the rotation vector  $\delta \hat{\boldsymbol{\lambda}}_k$  according to (1). The remaining state variables are linearly compensated using

$$\begin{aligned} \mathbf{p}_k^+ &= \mathbf{p}_k^- - \delta \hat{\mathbf{p}}_k \\ \mathbf{v}_k^+ &= \mathbf{v}_k^- - \delta \hat{\mathbf{v}}_k \\ \mathbf{b}_{a\ k}^+ &= \mathbf{b}_{a\ k}^- - \delta \hat{\mathbf{b}}_{a\ k} \\ \mathbf{b}_{\omega\ k}^+ &= \mathbf{b}_{\omega\ k}^- - \delta \hat{\mathbf{b}}_{\omega\ k} \end{aligned}$$

After the error correction procedure is completed, the EKF error estimates are reset. Therefore, linearization assumptions are kept valid and the attitude error rotation vector is stored in the  $\mathcal{R}_k^+$  matrix, preventing attitude error estimates to fall in singular configurations. At the start of the next computation cycle ( $t = t_{k+1}$ ), the INS attitude and velocity/position updates are performed on the corrected estimates ( $\boldsymbol{\lambda}_k^+, \mathbf{v}_k^+, \mathbf{p}_k^+$ ).

## 3 Aiding techniques

This section presents a new USBL/INS tightly-coupled integration technique that is developed to enhance error estimation in low-cost strapdown navigation systems with application to AUVs. To avoid the extensive use of an acoustic communication channel, it is assumed that the USBL acoustic array is installed on board the vehicle. For benchmark purposes, the more conventional loosely-coupled solution that relies on solving separately the triangulation and sensor fusion problems is presented. The comparison between both strategies resorts to a rigorous stochastic characterization of the acoustic sensors noise present in the round trip travel time measurements.

The direction and distance of the transponders in the loosely-coupled strategy are computed resorting to the planar approximation of the acoustic waves [9]. In [10], a closed-form method to estimate source's position using solely Time-Difference-Of-Arrival (TDOA) measurements is presented, without the planar wave approximation. However this method yields poor performance for USBL arrays compared to the method presented in this paper. In fact, due to noise levels and the proximity of the receivers on a USBL array, USBL positioning systems require travel time measurements to accurately estimate range between the transponders and the USBL array [11, 12, 13] whereas Direction-Of-Arrival (DOA) estimates are computed resorting to TDOA measurements.

The determination of the round trip travel time and the respective stochastic characterization are obtained resorting to pulse detection matched filters of acoustic signals modulated using spread-spectrum CDMA [11]. Two main error sources are identified: the first, common to all receivers, includes transponder-receiver relative motion time-scaling effects (Doppler effects and others) and errors in sound propagation velocity; the

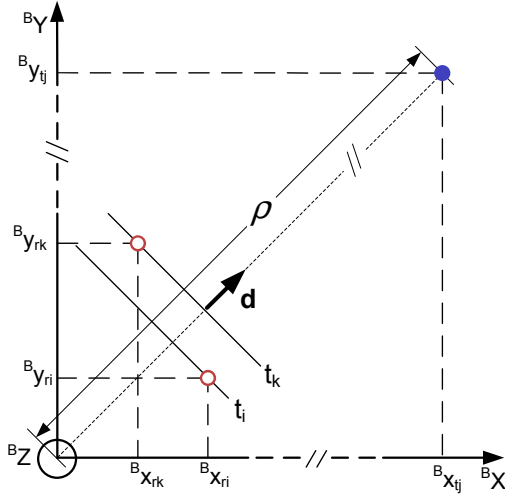


Figure 3: Planar wave approximation

second, corresponds to the differential quantization error induced by the acoustic system sampling frequency and the digital implementation of the detection algorithms. A method of estimation of TDOA and Scale-Difference-Of-Arrival (SDOA) with moving source and receivers is presented in [14]. However, SDOA effects can be neglected when using USBL arrays in underwater vehicles with low linear and angular velocity profiles as in the scope of this work.

With the purpose of attitude error compensation and to strengthen the overall system observability, Earth magnetic field readings, provided by an onboard magnetometer extra aiding device, are included in the proposed solution by means of an INS vector aiding methodology presented in [15].

### 3.1 Loosely-coupled USBL/INS

The loosely-coupled USBL/INS strategy uses the USBL device to obtain the direction and distance of the transponders to compute their relative positions expressed in Body frame. The USBL sub-system computes the range and direction of the transponders resorting to the planar approximation of the acoustic waves as in the classical approach presented in [9]. Consider the planar wave, the two acoustic receivers and the transponder depicted in Figure 3. The measurement of travel-time is obtained from the round trip travel time of the acoustic signals between the USBL array and the transponder  $2\bar{t}_i$  and is given by

$$t_{i,m} = \bar{t}_i + \varepsilon_c + \varepsilon_{d_i}$$

where  $\varepsilon_c$  represents the common mode noise for transponder  $j$  and  $\varepsilon_{d_i}$  is the differential noise for the  $j-i$  transponder-receiver pair (for the sake of simplicity, the index  $j$  is omitted in the equations).

Taking into account the planar wave approximation, it can be written that the TDOA between receivers  $i$  and  $k$  is given by

$$\delta^{(i,k)} = t_i - t_k = -\frac{1}{v_p} \mathbf{d}^T (\mathbf{}^B \mathbf{p}_{r_i} - \mathbf{}^B \mathbf{p}_{r_k}) \quad (6)$$

where  $v_p$  is the speed of sound in the water,  $\mathbf{}^B \mathbf{p}_{r_g}$  is receiver  $g$  ( $g = \{i, k\}$ ) position on Body frame and  $\mathbf{d}$  is the unit direction vector of transponder  $j$  ( $\|\mathbf{d}\|_2 = 1$ ).

The vector of TDOA between all possible combinations of  $N$  receivers is described, from (6)  $\{i = 1, \dots, N; k = 1, \dots, N; i \neq k\}$ , by

$$\Delta = [\delta^{(1,2)}_1 \quad \delta^{(1,3)}_2 \quad \dots \quad \delta^{(N-1,N)}_M]^T$$

and it can be generated by

$$\Delta = \mathbf{C} \mathbf{t}_m$$

where  $\mathbf{C}$  is a combination matrix and  $\mathbf{t}_m$  is the vector of time measurements from all receivers given by

$$\mathbf{t}_m = [t_{1,m} \quad t_{2,m} \quad \dots \quad t_{N,m}]^T$$

Thus, the least squares solution for the transponder's  $j$  direction  $\mathbf{d}$  is

$$\hat{\mathbf{d}} = -v_p \mathbf{S}^\# \mathbf{C} \mathbf{t}_m$$

where

$$\mathbf{S} = \begin{bmatrix} x_1 - x_2 & y_1 - y_2 & z_1 - z_2 \\ x_1 - x_3 & y_1 - y_3 & z_1 - z_3 \\ \vdots & \vdots & \vdots \\ x_{N-1} - x_N & y_{N-1} - y_N & z_{N-1} - z_N \end{bmatrix}$$

and

$$\mathbf{S}^\# = (\mathbf{S}^T \mathbf{S})^{-1} \mathbf{S}^T$$

Also resorting to the planar wave approximation, the range of transponder  $j$  to the origin of Body frame can be computed by averaging the range estimates from all receivers. The estimate for receiver  $h$  ( $h = \{1, \dots, N\}$ ) is given by

$$\hat{\rho}_h = v_p t_h + \mathbf{}^B \bar{\mathbf{p}}_{r_h}^T \mathbf{d} \quad (7)$$

Thus, averaging (7) for all  $N$  receivers yields

$$\hat{\rho} = \frac{1}{N} \sum_{h=1}^N (v_p t_h + \mathbf{}^B \bar{\mathbf{p}}_{r_h}^T \mathbf{d})$$

The relative position of a transponder  $j$  expressed in Body frame is then computed by

$$\mathbf{}^B \mathbf{p}_{e_j m} = \hat{\rho}_j \hat{\mathbf{d}}_j \quad (8)$$

and it can be described by

$$\mathbf{}^B \mathbf{p}_{e_j m} = \overline{\mathcal{R}}' (\mathbf{}^E \bar{\mathbf{p}}_{e_j} - \bar{\mathbf{p}}) + \mathbf{n}_{pr} \quad (9)$$

where  $\mathbf{}^E \bar{\mathbf{p}}_{e_j}$  is the transponder's position in Earth coordinate frame,  $\bar{\mathbf{p}}$  is the position of the Body frame origin in Earth frame and  $\mathbf{n}_{pr}$  represents the relative position measurement noise, characterized by taking into account the acoustic sensors noises and the USBL positioning system (8).

The estimate of the relative position of the transponder  $j$  in Body frame can be computed using the INS *a priori* estimates  $\mathcal{R}$  and  $\mathbf{p}$ , as follows

$$\mathbf{}^B \mathbf{p}_{e_j} = \mathcal{R}' (\mathbf{}^E \bar{\mathbf{p}}_{e_j} - \mathbf{p})$$

Using the position error definition (3), replacing the rotation matrix  $\bar{\mathcal{R}}$  by the attitude error  $\delta\boldsymbol{\lambda}$  approximation (5), and ignoring second order error terms, manipulation of (9) yields

$${}^B\mathbf{p}_{e_j m} = {}^B\mathbf{p}_{e_j} + \mathcal{R}'\delta\mathbf{p} + [\mathcal{R}'\delta\boldsymbol{\lambda}\times] {}^B\mathbf{p}_{e_j} + \mathbf{n}_{pr} \quad (10)$$

Using the properties of skew-symmetric matrices in (10) yields

$${}^B\mathbf{p}_{e_j m} = {}^B\mathbf{p}_{e_j} + \mathcal{R}'\delta\mathbf{p} - [{}^B\mathbf{p}_{e_j}\times] \mathcal{R}'\delta\boldsymbol{\lambda} + \mathbf{n}_{pr}$$

The measurement residual used as observation in the EKF is given by the comparison between the measured and the estimated relative positions, leading to

$$\delta\mathbf{z}_{pr} = {}^B\mathbf{p}_{e_j m} - {}^B\mathbf{p}_{e_j} = \mathcal{R}'\delta\mathbf{p} - [{}^B\mathbf{p}_{e_j}\times] \mathcal{R}'\delta\boldsymbol{\lambda} + \mathbf{n}_{pr}$$

### 3.2 Tightly-coupled USBL/INS

The new proposed tightly-coupled USBL/INS integration strategy exploits directly the acoustic array spatial information to calculate the distances from the transponders to each receiver on the USBL array, and feeds this information directly into the EKF.

Let the distance between transponder  $j$  and receiver  $i$  be given by

$$\bar{\rho}_{ji} = \left\| {}^E\bar{\mathbf{p}}_{e_j} - {}^E\bar{\mathbf{p}}_{r_i} \right\| = \left\| {}^E\bar{\mathbf{p}}_{e_j} - \bar{\mathbf{p}} - \bar{\mathcal{R}} {}^B\bar{\mathbf{p}}_{r_i} \right\| \quad (11)$$

The measurement of distance obtained from the round trip travel time of the acoustic signals between the USBL array and the transponders  $2\bar{t}_{ji}$ , is given by

$$\rho_{ji m} = \bar{\rho}_{ji} + v_p n_{t_{ji}} = v_p \bar{t}_{ji} + n_{\rho_{ji}} \quad (12)$$

where  $\bar{\rho}_{ji}$  represents the nominal distance from transponder  $j$  to receiver  $i$ ,  $n_{t_{ji}}$  is given by

$$n_{t_{ji}} = \varepsilon_{c_j} + \varepsilon_{d_{ji}}$$

where  $\varepsilon_{c_j}$  represents the common mode noise for transponder  $j$  and  $\varepsilon_{d_{ji}}$  is the differential noise for the  $j-i$  transponder-receiver pair.

Replacing (11) in (12), and using the position error definition (3) and the approximation in (5), results in

$$\rho_{ji m} = \left\| {}^E\bar{\mathbf{p}}_{e_j} - \mathbf{p} + \delta\mathbf{p} - \mathcal{R} {}^B\bar{\mathbf{p}}_{r_i} + [\delta\boldsymbol{\lambda}\times] \mathcal{R} {}^B\bar{\mathbf{p}}_{r_i} \right\| + n_{\rho_{ji}} \quad (13)$$

Taking into account the properties of skew-symmetric matrices, we have from (13) that  $\rho_{ji m}$  is given by

$$\rho_{ji m} = \left\| {}^E\bar{\mathbf{p}}_{e_j} - \mathbf{p} + \delta\mathbf{p} - \mathcal{R} {}^B\bar{\mathbf{p}}_{r_i} - [\mathcal{R} {}^B\bar{\mathbf{p}}_{r_i}\times] \delta\boldsymbol{\lambda} \right\| + n_{\rho_{ji}}$$

that is used as the observation equation in the EKF for each transponder-receiver pair.

Acoustic sensors noise and disturbances  $n_{t_{ji}}$  in (12) can be directly fitted in the EKF by means of the observation noise covariance matrix or augmenting the state vector to hold better stochastic description, thus avoiding time-consuming noise characterization procedures.

### 3.3 Attitude error compensation

The extra attitude measurement residual  $\delta\mathbf{z}_{mag} = ({}^B\mathbf{m}_m - {}^B\mathbf{m})$  is computed by comparing the Earth magnetic field readings, provided by the magnetometer

$${}^B\mathbf{m}_m = \bar{\mathcal{R}}' {}^E\bar{\mathbf{m}} + \mathbf{n}_m$$

with the INS estimate

$${}^B\mathbf{m} = \mathcal{R}' {}^E\bar{\mathbf{m}}$$

Replacing the rotation matrix  $\bar{\mathcal{R}}$  by the attitude error  $\delta\boldsymbol{\lambda}$  approximation (5), yields

$$\begin{aligned} {}^B\mathbf{m}_m &= \mathcal{R}' [\mathbf{I}_{3\times 3} + [\delta\boldsymbol{\lambda}\times]] {}^E\bar{\mathbf{m}} + \mathbf{n}_m \\ &= \mathcal{R}' {}^E\bar{\mathbf{m}} - \mathcal{R}' [{}^E\bar{\mathbf{m}}\times] \delta\boldsymbol{\lambda} + \mathbf{n}_m \end{aligned}$$

resulting in a attitude measurement residual that is given by

$$\delta\mathbf{z}_{mag} = -\mathcal{R}' [{}^E\bar{\mathbf{m}}\times] \delta\boldsymbol{\lambda} + \mathbf{n}_m$$

For further details the reader is referred to [15].

### 3.4 Observability analysis

An observability analysis of both strategies was conducted resorting to the observability theorem [16]. The linear time varying discrete system given by

$$\begin{cases} \mathbf{x}(k+1) &= \boldsymbol{\phi}(k+1, k)\mathbf{x}(k) + \mathbf{B}(k)\mathbf{u}(k) \\ \mathbf{z}(k) &= \mathbf{H}(k)\mathbf{x}(k) + \mathbf{D}(k)\mathbf{u}(k) \\ \mathbf{x}(k_0) &= \mathbf{x}_0, \mathbf{x}(k) \in \mathbb{R}^{n\times 1}, \mathbf{z}(k) \in \mathbb{R}^{p\times n} \end{cases}$$

is said to be completely observable on  $[k_0, k_f]$ , with  $k_f \geq k_0 + 1$ , if and only if

$$\text{rank } \mathbf{O}(k_0, k_f) = n$$

where  $\mathbf{O}(k_0, k_f)$  is called observability matrix and is given by

$$\mathbf{O}(k_0, k_f) = \begin{bmatrix} \mathbf{H}(k_0) \\ \mathbf{H}(k_0+1)\boldsymbol{\phi}(k_0+1, k_0) \\ \vdots \\ \mathbf{H}(k_f-1)\boldsymbol{\phi}(k_f-1, k_0) \end{bmatrix}$$

Furthermore, the rank of the observability matrix indicates the number of observable variables on the system.

Observability analysis are presented in Table 1 for observation of USBL measurements and in Table 2 for observation of USBL measurements and magnetometer aiding, with a maximum of 15 observable variables. As expected, both strategies attained the same observability results.

Analysis of this results revealed that either stopped or along a straight line path, full observability is only achieved using at least three transponders (on a non-singular geometry) or two transponders and a magnetometer. Moreover, along curves two transponders or one transponder and a magnetometer are sufficient to achieve full observability. Interestingly enough, this analysis revealed that specific in-flight maneuvers like

Table 1: Observability results with USBL measurements

Maneuver	Transponders		
	1	2	3
Stopped	11	14	15
Straight line	11	14	15
Curve	13	15	15
Straight line → Curve	15	15	15

Table 2: Observability results with USBL measurements and magnetometer aiding

Maneuver	Transponders	
	1	2
Stopped	14	15
Straight line	14	15
Curve	15	15
Straight line → Curve	15	15

transitions between straight paths to curves, excite the non-observable directions of the system turning the filter to full observability, as discussed in [17, 18]. Recent work in [15, 19, 20] has been directed towards the inclusion of vehicle dynamic information to strengthen the system observability.

## 4 Simulation results

In this section the performance of the USBL/INS loosely and tightly-coupled strategies are compared in simulation, resorting to a rigorous stochastic characterization of the round trip travel time of the acoustic signals.

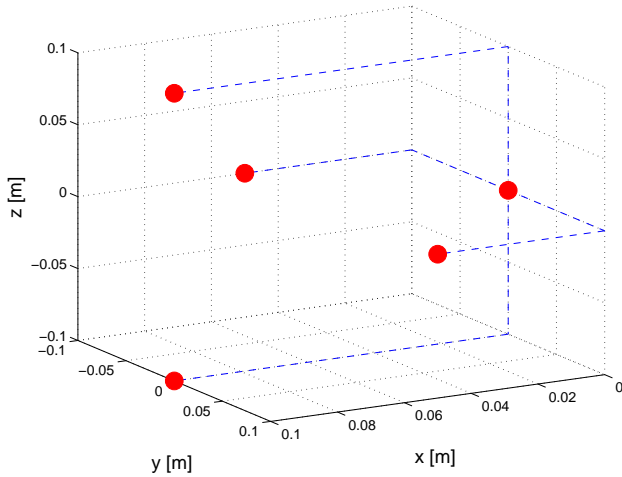
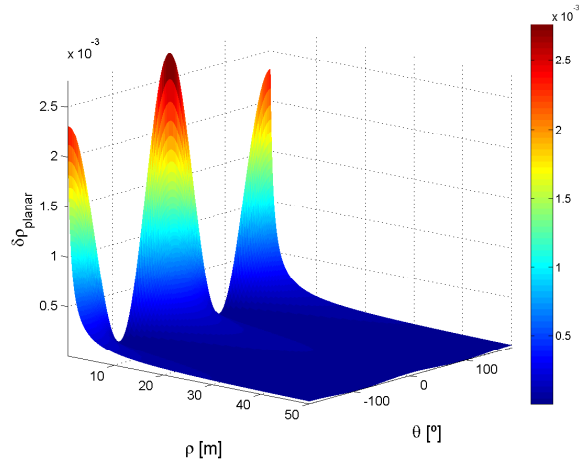
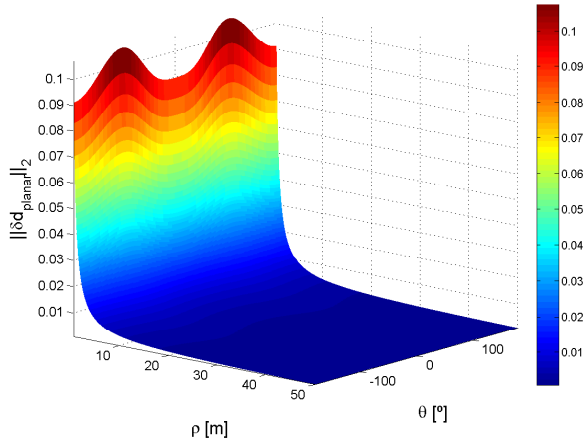


Figure 4: Receivers installation geometry

The planar wave approximation is validated using five receivers installed on the vehicle, in the configuration depicted in Figure 4. The approximation error is presented in Figure 5, where



a) Range



b) Direction

Figure 5: Planar wave approximation error (null elevation:  $\phi = 0$ )

$\delta \mathbf{d}_{planar} = \mathbf{d} - \hat{\mathbf{d}}_{planar}$ ,  $\delta \rho_{planar} = \rho - \hat{\rho}_{planar}$ ,  $\mathbf{d} = [\cos \phi \sin \theta, \cos \phi \cos \theta, \sin \phi]^T$ ,  $\theta$  is the bearing and  $\phi$  the elevation angle of the transponder in Body frame. As the distance between the USBL array and the transponder increases, the error of the planar wave approximation converges to zero, as expected.

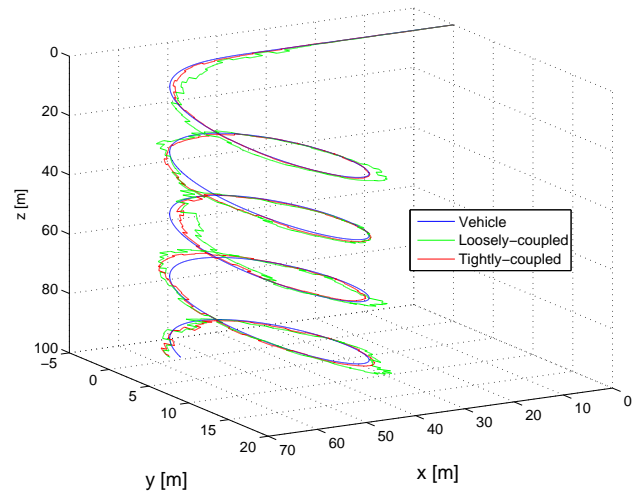


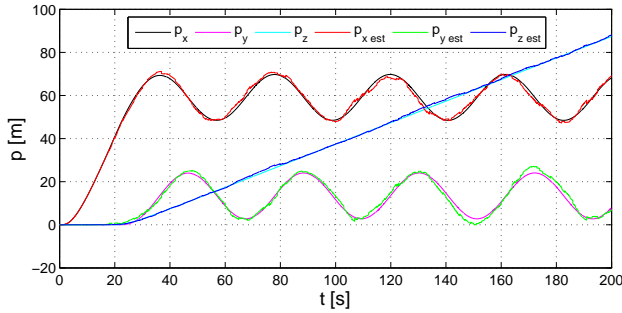
Figure 6: USBL/INS estimated and vehicle trajectory

The performance of both strategies is assessed in simulation, using one magnetometer and five receivers installed on the vehicle, in the configuration depicted in Figure 4, and one transponder located at  $[100, 0, 0]^T$  m. The vehicle follows a trajectory composed by a initial straight line with non-null acceleration followed by a descending helix represented in Figure 6.

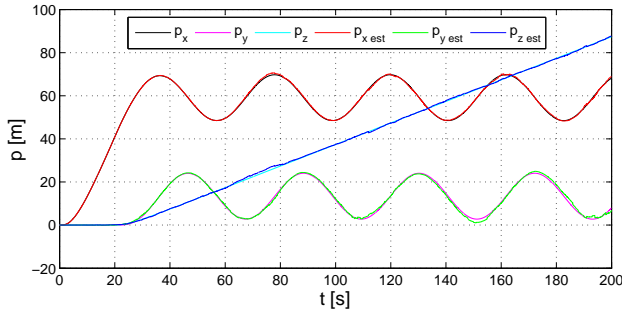
The INS high-speed algorithm is set to run at 100 Hz and the normal-speed algorithm is synchronized with the EKF, both executed at 50 Hz. The USBL array provides measurements at 1 Hz. The noise and bias characteristics of the sensors are presented in Table 3.

Table 3: Sensor errors

Sensor	Bias	Noise Variance
Rate gyro	0.05 °/s	$(0.02 \text{ °/s})^2$
Accelerometer	10 mg	$(0.6 \text{ mg})^2$
Magnetometer	-	$(1 \text{ } \mu\text{G})^2$
Acoustic sensors	Bias	Noise Variance
Common mode	-	$(50 \text{ } \mu\text{s})^2$
Differential mode	-	$(5 \text{ } \mu\text{s})^2$



a) Loosely-coupled strategy

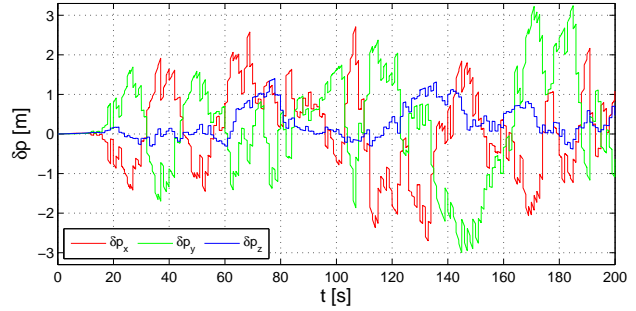


b) Tightly-coupled strategy

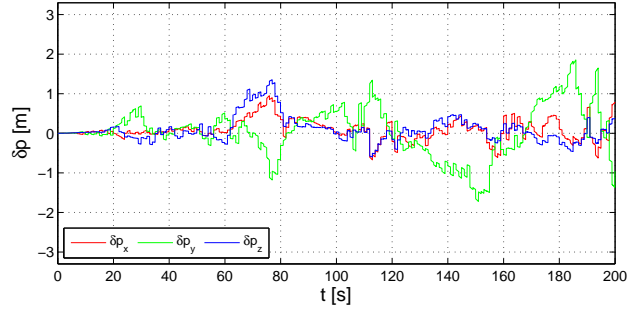
Figure 7: Position estimation

The vehicle trajectory estimated by the overall navigation system for the proposed strategy and the loosely-coupled strategy is shown in Figure 6. Position estimates for both strategies are plotted in Figure 7 where the proposed strategy improvements are evident.

The performance enhancement of the proposed strategy is more clear from the position estimation errors presented in Figure 8, and summarized in Table 4 for both cases. Orientation estimation errors are also lower for the tightly-coupled strategy.



a) Loosely-coupled strategy



b) Tightly-coupled strategy

Figure 8: Position estimation errors

Table 4: Summary of estimation errors (RMS)

Strategy	$\delta p_x$ [m]	$\delta p_y$ [m]	$\delta p_z$ [m]
Loosely-coupled	1.07	1.29	0.48
Tightly-coupled	0.27	0.63	0.33
Strategy	$\delta \psi$ [°]	$\delta \theta$ [°]	$\delta \phi$ [°]
Loosely-coupled	0.0278	0.0271	0.0284
Tightly-coupled	0.0145	0.0139	0.0151

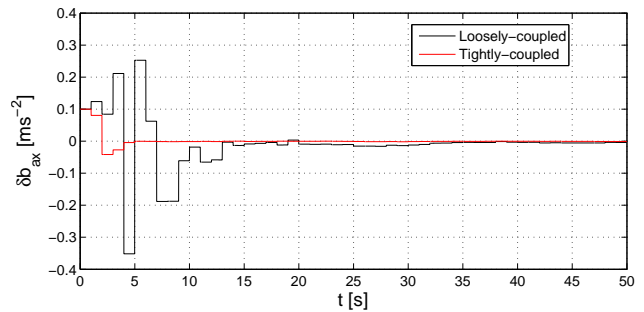


Figure 9: Bias misalignment

To assess the enhanced capability of the proposed tightly-coupled technique on tackling initial alignment errors, an additional simulation was run for an initial misalignment of 10 mg on Body frame x-axis accelerometer bias with the vehicle describing a descending helix. As evidenced by Figure 9, the tightly-coupled strategy alignment errors converge faster to zero achieving also better steady-state bias estimates.

## 5 Conclusions

A new USBL tightly-coupled integration technique to enhance error estimation in low-cost strapdown INS with application to underwater vehicles was proposed. The acoustic array spatial information is directly exploited resorting to an EKF implemented in a direct feedback configuration. The performance of the overall navigation system was compared with the more commonly used loosely-coupled solution, from where the enhancement on the position and attitude estimates became clear. Future work will focus on an indepth characterization of the round trip travel time error sources and on the implementation of the proposed tightly-coupled USBL/INS architecture in a low-power consumption DSP hardware architecture.

## References

- [1] A. Pascoal, P. Oliveira, and C. Silvestre *et al.*, “Robotic Ocean Vehicles for Marine Science Applications: the European ASIMOV Project,” in *Proceedings of the Oceans 2000*, Rhode Island, USA, September 2000.
- [2] B. Jalving, K. Gade, O.K. Hagen, and K. Vestgard, “A toolbox of aiding techniques for the HUGIN AUV integrated inertial navigation system,” in *Proceedings of the Oceans 2003*, San Diego CA, USA, September 2003.
- [3] F. Napolitano, F. Cretollier, and H. Pelletier, “GAPS, combined USBL + INS + GPS tracking system for fast deployable and high accuracy multiple target positioning,” in *Proceedings of the Oceans 2005 - Europe*, Brest, France, June 2005.
- [4] S. Sukkariéh, *Low Cost, High Integrity, Aided Inertial Navigation Systems for Autonomous Land Vehicles*, Ph.D. thesis, The University of Sydney, March 2000.
- [5] P.G. Savage, “Strapdown Inertial Navigation Integration Algorithm Design Part 1: Attitude Algorithms,” *AIAA Journal of Guidance, Control, and Dynamics*, vol. 21, no. 1, pp. 19–28, January-February 1998.
- [6] P.G. Savage, “Strapdown Inertial Navigation Integration Algorithm Design Part 2: Velocity and Position Algorithms,” *AIAA Journal of Guidance, Control, and Dynamics*, vol. 21, no. 2, pp. 208–221, March-April 1998.
- [7] K.M. Roscoe, “Equivalency Between Strapdown Inertial Navigation Coning and Sculling Integrals/Algorithms,” *AIAA Journal of Guidance, Control, and Dynamics*, vol. 24, no. 2, pp. 201–205, 2001.
- [8] K.R. Britting, *Inertial Navigation Systems Analysis*, John Wiley & Sons, Inc., 1971.
- [9] J. Yli-Hietanen, K. Kalliojarvi, and J. Astola, “Low-Complexity Angle of Arrival Estimation of Wideband Signals Using Small Arrays,” in *Proceedings 8th IEEE Signal Processing Workshop on Statistical Signal and Array Processing*, 1996.
- [10] J.O. Smith and J.S. Abel, “The Spherical Interpolation Method of Source Localization,” *IEEE Journal of Oceanic Engineering*, vol. 12, no. 1, pp. 246–252, 1987.
- [11] T.C. Austin, “The application of spread spectrum signaling techniques to underwater acoustic navigation,” in *Proceedings of the 1994 Symposium on Autonomous Underwater Vehicle Technology, 1994. AUV '94*, 1994.
- [12] F.V.F. de Lima and C.M. Furukawa, “Development and testing of an acoustic positioning system - description and signal processing,” in *Proceedings of the IEEE 2002 Ultrasonics Symposium*, 2002.
- [13] P.H. Milne, *Underwater Acoustic Positioning Systems*, Gulf Pub. Co., 1983.
- [14] Y.T. Chan and K.C. Ho, “TDOA-SDOA Estimation with Moving Source and Receivers,” in *Proceedings of the ICASSP 2003*, Hong Kong, 2003.
- [15] J.F. Vasconcelos, P. Oliveira, and C. Silvestre, “Inertial Navigation System Aided by GPS and Selective Frequency Contents of Vector Measurements,” in *Proceedings of the AIAA Guidance, Navigation, and Control Conference (GNC2005)*, San Francisco, USA, August 2005.
- [16] W. Rugh, *Linear System Theory*, Prentice-Hall, second edition, 1996.
- [17] D. Goshen-Meskin and I. Bar-Itzhack, “Observability Analysis of Piece-Wise Constant Systems - Part I: Theory,” *IEEE Transactions On Aerospace and Electronic Systems*, vol. 28, no. 4, pp. 1056–1067, 1992.
- [18] D. Goshen-Meskin and I. Bar-Itzhack, “Observability Analysis of Piece-Wise Constant Systems - Part II: Application to Inertial Navigation In-Flight Alignment,” *IEEE Transactions On Aerospace and Electronic Systems*, vol. 28, no. 4, pp. 1068–1075, 1992.
- [19] M. Koifman and I. Bar-Itzhack, “Inertial Navigation System Aided by Aircraft Dynamics,” *IEEE Transactions on Control Systems Technology*, vol. 7, no. 4, pp. 487–493, 1999.
- [20] X. Ma, S. Sukkariéh, and J. Kim, “Vehicle Model Aided Inertial Navigation,” in *Proceedings of the IEEE Intelligent Transportation Systems*, Shanghai, China, 2003.